PARENTAL MELT COMPOSITION OF THE NORTHWEST AFRICA 13669 NAKHLITE FROM PYROXENE AND OLIVINE-HOSTED MELT INCLUSIONS. S. Ramsey[1], A. Ostwald[1], A. Udry[1], J. M. D. Day[2]. [1]Department of Geoscience, University of Nevada, Las Vegas, Las Vegas NV, USA; ramses3@unlv.nevada.edu. [2]Scripps Institution of Oceanography, University of California San Diego, La Jolla, CA, USA.

Introduction: Meteorites are the only sample-type we possess from Mars, which makes their study crucial to understanding the evolution of martian magmatic and volcanic processes. Nakhlites are one of the three main groups of martian meteorites and are cumulate clinopyroxene-rich rocks linked by shared crystallization ages (1340 ± 40 Ma) and cosmic ray exposure ages (11 ± 1.5 Ma) [1–2]. Given their shared ages and similar textures and mineralogy, the nakhlites are the largest coherent suite of igneous rocks from a common provenance on any planetary body besides the Moon and Earth [2]. Nakhlites are likely to be vital for understanding the evolution of magmatic plumbing systems on Mars.

One method of interrogating the relationship between cumulate rocks is by studying their parental melt compositions using melt inclusions (MI), or small pockets of melt entrapped, while a crystal is growing [e.g., 3]. Here we present calculated parental melt compositions derived from olivine and pyroxene-hosted MI to assess the petrogenesis of NWA 13669 and its relation to other nakhlites.

Methods: *Major, minor, and trace element analyses:* Major and minor elemental analyses for four pyroxene and one olivine-hosted MI in NWA 13669 were conducted *in situ* using a *JEOL* JXA-8900 EPMA housed at the University of Nevada, Las Vegas (UNLV). Phases in polycrystalline MI were measured individually with a beam spot size of 1 µm if large enough (>2 µm), otherwise a defocused beam size of 5 µm was used to estimate a bulk analysis of multiple phases. A beam size of 10 µm and probe current of 10 nA was used for glass inclusions and glassy material in polycrystalline inclusions to prevent volatilization and Na migration. Trace element analyses were conducted *in situ* using a NWR 139 laser ablation system coupled to an iCAP Qc quadrupole ICP-MS at UNLV. The laser was operated at 15 Hz and a photon fluence of ~3 J/s was maintained throughout analyses. A spot size of 50 µm was used to measure the bulk composition of all MI phases. Standardization was done using the NIST 610 glass and BHVO-2 and LA-ICP-MS data was reduced using *iolite 4* [4]. All analyses were then corrected for host phase contributions.

Parental trapped liquid calculations: Modal abundances of MI were calculated using back scattered electron images and *ImageJ*. The parental bulk composition was determined for each inclusion by adjusting EPMA data for the modal and density contribution of each present phase. For olivine-hosted MI, the effects of rehomogenization were corrected with *Petrolog3* [5], which requires an estimate for initial Fe content (FeO_T) of the parental trapped liquid (PTL). We used literature estimates of 28.9 wt.% [6] and 22.2 wt.% [7] for nakhlites, following the methodology of [8]. Cation exchange between MI and pyroxene hosts were corrected with *Rhyolite-MELTS* [9], where we adjusted the modal abundances of each element present in the PBCs until a pyroxene with the observed host composition was in equilibrium. This calculated composition was taken as the PTL for the inclusion.

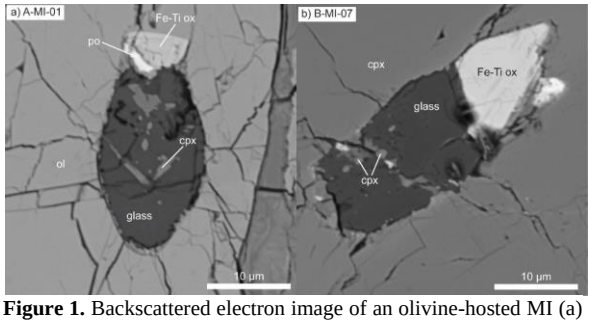

Figure 1. Backscattered electron image of an olivine-hosted MI (a) and a pyroxene-hosted MI (b) in NWA 13669 analyzed in this study. Cpx = clinopyroxene, ol = olivine, po = pyrrhotite.

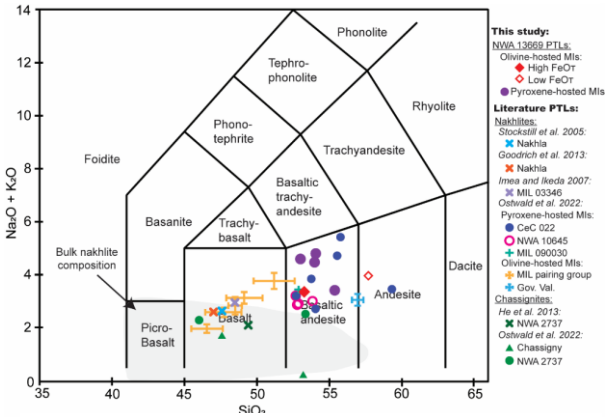

Figure 2. Total alkali (Na_2O+K_2O) versus silica diagram for NWA 13336 PTL compositions, plotted with PTL compositions from previous studies. Grey envelope indicates bulk nakhlite compositions [2].

Results: *Melt inclusions petrography:* All MI analyzed in NWA 13669 are small (<40 µm). The single olivine-hosted MI (A-MI-01) was elliptical and polycrystalline (Fig. 1). Clinopyroxene microlites (≤2 µm) are set in glass, with a modal abundance of 89% glass and 11% clinopyroxene. Pyroxene-hosted inclusions are mostly glassy and elongate in shape (Fig. 1), primarily consisting of varying amounts of glass (34–94%) and cognate Fe-Ti oxides (6–51%).

Parental trapped liquid compositions: The modeled PTL for our olivine-hosted MI (Fig. 2), varies

depending on the initial FeO_T. Using a low FeO_T value [7] yielded an andesitic PTL with 58 wt.% SiO_2, 10 wt.% Al_2O_3, 18 wt.% FeO, 5 wt.% Fe_2O_3, and 2 wt.% MgO. A higher FeO_T [6] value produced a basaltic-andesitic PTL with 53 wt.% SiO_2, 8 wt.% Al_2O_3, 22 wt.% FeO, 8 wt.% Fe_2O_3, and 2 wt.% MgO. Modeled pyroxene-hosted MI PTLs are basaltic-andesite (Fig. 2) and range from 53 to 55 wt.% SiO_2, 6 to 10% Al_2O_3, 16 to 21 wt.% FeO_T, and 3.2 to 4.8 wt.% MgO. Overall alkali content in PTLs for all inclusions is enriched and ranges from 2–4 wt.% Na_2O and 1–3 wt.% K_2O. These PTL compositions and alkali enrichments are in general agreement with those calculated by [8] for nakhlites.

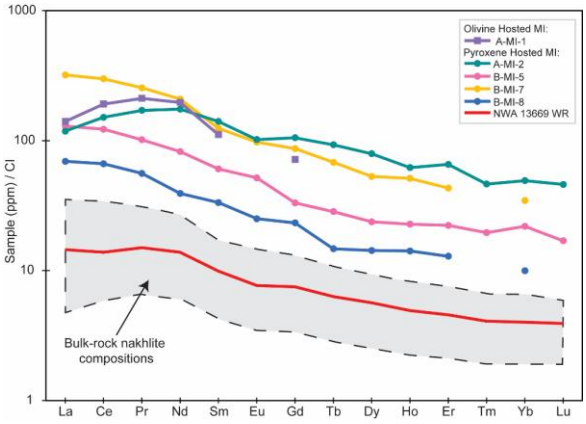

Figure 3. CI-normalized [20] REE abundances in NWA 13669 MI and NWA 13669 whole rock. Grey envelope indicates bulk nakhlite compositions [2].

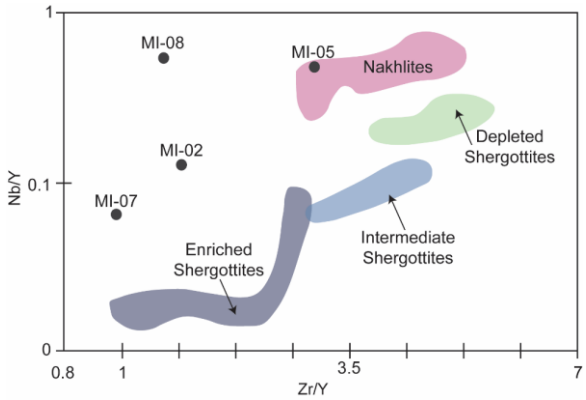

Figure 4. Zr/Y and Nb/Y diagram with NWA 13669 MI data with bulk nakhlites and shergottites ranges (envelopes). Adapted from [10].

Trace element abundances in MI are more enriched (>10 × CI) in rare earth elements (REE) than the whole rock (Fig. 3), but broadly parallel the whole rock REE pattern of NWA 13669 and the whole rock REE patterns of other nakhlites. Northwest Africa 13669 MI exhibit a notable light REE enrichment and pyroxene-hosted inclusions have varying degrees of REE enrichment.

Discussion: Nakhlites are low-degree partial melts from a long-term incompatible trace element depleted mantle source (e.g., [2, 10]), but have undergone late-stage modification by Cl- and LREE-rich fluids [11]. Our whole rock [12] and MI compositions (Fig. 3) suggest NWA 13669 sampled a single depleted mantle source that is the same as other nakhlites given the broad parallelism between REE patterns for MI and the nakhlite whole rock compositions (Fig. 3).

Ratios of trace elements (e.g., Zr/Y, Nb/Y) between MI are variable, and do not plot within the nakhlite bulk rock field, apart from MI-05 (Fig. 4). Scatter has been observed in a previous nakhlite study [13] and likely indicates a post-entrapment process, such as re-equilibration between the host phase and MI has occurred. Re-equilibration, when combined with multiple parental melt compositions across the nakhlite suite, suggests magma generation was long-lived and the cumulus nakhlite phases underwent magma storage [13]. The trace element scatter (Fig. 4) also indicates the parent melt responsible for NWA 13669 likely had a period of residence time before entrainment and emplacement at or near the martian surface, likely within a crystal mush. Storage in a crystal mush would allow the observed diffusive re-equilibration between host and MI to occur, which is consistent with the current understanding of terrestrial magma chamber dynamics [e.g., 14].

Northwest Africa 13669 PTLs are enriched in alkali elements (e.g., K_2O and Na_2O). Alkali enrichment due to boundary layer effects is possible in small inclusions [15], but we do not see a correlation between size and alkali content as would be expected if enrichments were caused by entrapping a boundary layer. Potassium enrichments in nakhlite and shergottite parental melts have been previously noted by [6–8] and [16–17], and [6] suggested the K_2O enrichment could be due to metasomatism of the nakhlite source before melting. Alkali enrichments have also been detected in the NWA 7034 regolith breccia [18] and in *in situ* measurements on Mars by rovers [e.g., 19], implying alkali-rich magmatism from low degree partial melting or melting of a metasomatized source, may be prevalent on Mars.

References: [1] Udry et al. (2020) *JGR: Planets*, 125, 1–34. [2] Udry and Day (2018) *GCA*, 238, 292–315. [3] Stockstill et al. (2005) *Met. Planet. Sci*., 48, 2371–2405. [4] Paton et al. (2011) *J. An. Atomic Spec*. 26, 2508–2518. [5] Danyushevsky and Plechov (2011) *GGG*, 12, No. 7. [6] Goodrich et al. (2013) *Met. Planet. Sci*., 48, 2371–2405. [7] Imae and Ikeda (2007) *Met. Planet. Sci*., 42, 171–184. [8] Ostwald et al. (2020) *LPSC LI* abstract #2213. [9] Gualda et al. (2012) *J. of Pet*., 53, 875–890. [10] Day et al. (2018) *Nat. Comm*., 9, 4799. [11] McCubbin et al. (2013) *Met. Planet Sci*. 48, 819–853. [12] Ramsey et al. (2022) *LPSC LIII* abstract #1127. [13] Ostwald et al. (2022) *LPSC LIII* abstract #1206. [14] Weiser et al. (2019) *Nat. Comm*., 10, 1–11. [15] Lu et al. (1995) *J. of Geology*, 48, 1572–1589. [16] O'Neal et al. (2022) *LPSC LII* abstract #1065. [17] Combs et al. (2019) *GCA*, 266, 435–462. [18] Agee et al. (2013) *Science*, 339, 780–785. [19] Thompson et al. (2016) *JGR: Planets* 121, 1981–2003. [20] McDonough and Sun (1995) *Chem. Geo*. 120, 223–253.